Bulletin of Earthquake Engineering (2024) 22:2139–2171
https://doi.org/10.1007/s10518-023-01849-x

ORIGINAL ARTICLE

Seismic pounding of adjacent buildings considering torsional effects

Esra Ozer[1]

Received: 29 July 2023 / Accepted: 20 December 2023 / Published online: 20 January 2024
© The Author(s) 2024

Abstract
This study aims to evaluate pounding effects in fixed-base models by considering torsional irregularity. For this purpose, 8 different adjacent building combinations were created by using 3-dimensional 5- and 9-story building models. In adjacent building models, the most critical situation was determined by evaluating the gap distance, different sequences of the same building models and regular or irregular plan view and if the structures are irregular, their eccentricity cases relative to each other. Nonlinear behavior of structural elements was taken into account for examine the change in the seismic behavior of structural elements due to pounding and torsion effects. The nonlinear time history analysis of the adjacent models was performed for 11 pairs of spectrum compatible ground motion recordings in the SAP2000 program. The results of 176 different analyzes show that the displacement demand, interstory drift ratio, damage ratio and torsional irregularity coefficient values tend to increase in general with the combined effects of pounding and torsion. The absolute maximum and most critical values of the relevant parameters were calculated in irregular structures with pounding where the eccentricity of buildings is in the same direction and same side. In addition, the large standard deviation of the result values according to the ground motion records indicates that care should be taken in choosing the number of ground motion records.

Keywords Seismic pounding · Torsion behavior · Adjacent buildings · Eccentric pounding · Nonlinear time history analysis

1 Introduction

The areas with dense population are generally encountered adjacent buildings with insufficient gap distances because of commercial and architectural reasons. In the study conducted by Doğan and Günaydin (2009), it is stated that 64% of the buildings in Eskişehir have insufficient gap distance. The insufficient gap may cause adjacent structures to collide with each other under seismic loads. This situation, which causes severe damage or even collapse in buildings on a local or global scale, constituted 40% of life safety performance

✉ Esra Ozer
esra.ozer@gop.edu.tr

[1] Department of Civil Engineering, Tokat Gaziosmanpasa University, 60250 Tokat, Turkey

level and 15% of total collapses in the Mexico earthquake (Miari et al. 2019; Rosenblueth and Meli 1986; Degg 1992). This pounding effect with undeniable scale is tried to be prevented with various formulations in many international design regulations or decrease of effects. However, the gap distances recommended in the regulations to prevent collisions are generally insufficient due to the pounding behavior complicated by many factors such as torsion, soft story, weak story, soil–structure interaction, story height, structure height of adjacent buildings, pounding configuration (floor-to-floor collision, floor-to-column collision) (Miari et al. 2019; Miari and Jankowski 2022; Jeng and Tzeng 2000; Cole et al. 2010), nonlinear behavior, ground motion excitation angle to buildings and the frequency content of the ground motion (Mavronicola et al. 2017).

When the previous studies on the subject are examined; many studies have been conducted on modeling pounding behavior between adjacent structures (stereomechanical or force-based approach) (Ye et al. 2009). Although there are also many studies on the pounding effect, the building models used are generally single-degree-of-freedom (SDOF) (Wada et al. 1984; Anagnostopoulos 1988; Jing and Young 1991; Davis 1992; Chau and Wei 2001) or simplified multi-degree-of-freedom systems (MDOF) (Naderpour et al. 2017; Zhai et al. 2015), and the linear effects in the collision direction are only considered. However, recent studies in the field of earthquake-induced pounding between three-dimensional(3D) adjacent structures have revealed that neglecting possible local inelastic effects in potential impact situations leads to non-conservative building design and building seismic evaluation that can become inaccurate in some cases (especially inter-story pounding configuration) (Karayannis and Favvata 2005a, 2005b; Cayci and Akpinar 2021; Flenga and Favvata 2021, 2023; Karayannis and Naoum 2018). Because the pounding effect is a parameter that may redistribute the local inelastic demands of structural members (Flenga and Favvata 2021). Furthermore, Freddi et al. (2017) was point out that verification of both global and local capacities when seismic performance assessment of structures is performed through deterministic inelastic analysis procedures are needed. In the study conducted by Anagnostopoulos (1988), it was also stated that the outer column elements exposed to pounding tend to suffer more than the inner column members.

In other studies, the pounding behavior of the colliding buildings was examined according to parameters such as mass, story height, building height, period value. These studies concluded that the farther the values of these parameters of the two buildings from each other, the more critical the collision is generally (Zhai et al. 2015; Jankowski 2009; Karayannis and Naoum 2018). Although most of the studies have developed a general approach about the effects of symmetrical collision in typical buildings, the results of studies have moved away from a realistic approach due to ignoring the contact geometry of the colliding surfaces, the structural eccentricity, the movement in the direction orthogonal to the collision direction and the friction force.

Different from these, various approaches have been developed regarding the distance of gap that should be left between 3D buildings considering the colliding buildings are seismic isolated or not (Mavronicola et al. 2020; Rayegani and Nouri 2022; Pant and Wijeyewickrema 2012; Barros et al. 2013; Mazza and Labernarda 2020; Ye et al. 2009), taking into account or not the soil–structure interaction (Ghandil and Aldaikh 2017; Cayci and Akpinar 2021) or modeling them as conventional fixed-base (Lopez-Garcia and Soong 2009). In a study conducted by Favvata (2017), it was stated that the minimum gap distance that should be left between reinforced concrete buildings with different story heights depends on the limit condition taken into account and the seismic hazard level. Flenga and Favvata has been developed another approach based on the probabilistic evaluation of inelastic local demands of structural members (Flenga and Favvata 2021). For this purpose,

different linear and bilinear regression analyzes were performed. Although the results obtained are limited to the fragility curves of a reinforced concrete building, it is the first realistic probabilistic study in this field. Because the local inelastic behavior of structural elements in adjacent models with the same and different story heights is taken into account and evaluated probabilistic, simultaneously.

On the other hand, it was first time by Karayannis and Favvata (2005a), stated by that pounding effect of adjacent buildings with different story heights situation was more critical than the collision behavior of adjacent buildings with the same story height. Additionally, the outer columns of the taller building that were subject to collision were modeled with distributed plastic hinges in order to examine the possible nonlinear effects of the collision in more detail and realistic. In line with the results obtained, it was stated that the external columns hitting the slab may show local collapse behavior by being exposed to shear forces above their capacity and ductility demands above their capacity, in case of strong ground motion due to nonlinear behavior (Favvata et al. 2009; Karayannis and Favvata 2005a, b). It has been concluded that this situation (floor-to-column collision) may disrupt the stability of the building and even bring the system to the collapse performance level (Jing et al. 2023). For this reason, this effect is defined as an important reason for ensuring structural stability (Eurocode-8 2008). Similarly, this critical effect (floor-to-column collision) was examined by Shakya and Wijeyewickrema (2009) by taking into account the soil structure interaction under near fault and far fault effects. The result obtained showed that the demand values obtained in reinforced concrete buildings with different story heights under near fault movements are even more critical when the soil–structure interaction is not considered. Efraimiadou et al. (2013) examined the pounding effect on 9 different regular and irregular structures with the same and different story heights. It has been stated that while pounding behavior may be beneficial for one of the buildings, it is harmful for the other and this harm has been more than the benefit. For this reason, the use of energy-absorbing materials to prevent collisions and energy dissipation devices that reduce the impact of collisions have been the focus of other studies, recently (Mavronicola et al.2020; Rayegani and Nouri 2022; Abdel Raheem 2014). Unlike other studies Jiang et al. (2022) stated that the impact forces in case of floor-to-floor impact are greater than inter-story impact according to experimental and analytical studies.

On the other hand, in many of these studies, it has been stated that torsion amplifications can increase due to pounding, torsion behavior is an irregularity situation that we encounter much more frequently than pounding, and the pounding behavior becomes more complex with torsion (Karayannis and Naoum 2018; Chau et al. 2004; Wei et al. 2009; Fiore et al 2013; Kuo 1974; Tabatabaei 2011; Jing et al. 2023). However, studies examining both pounding effects and torsional behavior have been quite limited.

Combined of torsion and pounding effects were first studied by Leibovich et al. (1996) on two symmetrical SDOF models when the gap distance between buildings is variable. Papadrakakis et al. (1996) and Mouzakis and Papadrakakis (2004) developed 3-dimensional (3D) collision models. Hao and Shen (2001) investigated the appropriate gap distance for two SDOF towers with torsional behavior. In the studies conducted by Gong and Hao (2005), torsional pounding under bi-directional earthquake loading on symmetric and asymmetric SDOF models was examined. Wang et al. (2009) investigated the nonlinear torsional pounding behavior on SDOF tower models. In their study, Karayannis and Naoum (2018) examined asymmetric pounding on multi-story structures with three ground motion records. The asymmetry was achieved by the fact that the starting and ending points of the buildings in the direction orthogonal to the collision are not aligned (withdraw, not on the same row, or asymmetry in the interaction area). Mazza and Labernarda (2022), on the

other hand, investigated the pounding behavior of irregular buildings in plan. One of the 3D structures is modeled with fixed base and the other with a base isolator.

In the adjacent systems, it is quite important to consider the torsion effects on structure with pounding, especially on eccentric building due to seismic response of the structure is affected by pounding, torsion and their combined effects. Thus, in this study, the torsion and pounding behavior of symmetrical and asymmetrical with the same start and end alignment 3D fixed-base models (which are most common in city centers), is examined by taking into account the nonlinear behavior of the structural elements for more realistic approach. The nonlinear behavior is reflected in the model through plastic hinges defined at both ends of the beam and column elements. Additionally, the most critical situation in terms of torsional and pounding amplifications was also determined by evaluating the asymmetry of the asymmetrical buildings relative to each other. For the combined examination of torsion and pounding, symmetrical and non-pounding mid-rise 5- and 9-story reinforced concrete (RC) frame models were taken as reference. Asymmetric and adjacent models were derived from reference models. The dynamic analysis of the models in the time history using 11 spectrum compatible ground motion pairs was made in the SAP2000 program. As a result of the analysis, the changes in the parameters of maximum displacement, interstory drift ratio, damage scatter and torsion coefficient were compared for pounding/without pounding and symmetric/asymmetric models.

2 Building properties and modeling

2.1 Properties of regular and irregular structures

In the scope of the study, completely symmetrical 5 and 9-story two reference buildings without any structural irregularities were modeled separately. 2018 Turkish Building Earthquake Code (TBEC-2018) was taken into account in the modeling of the 3-dimensional (3D) reference buildings. The mass center (CM) and the rigidity center (CR) of the fixed-base models coincide with each other in the direction of both principal axes. Concrete compressive strength is 30 MPa, longitudinal and transverse reinforcement yield strength is 420 MPa. Stress–strain relationship for reinforcement, concrete and confined concrete were given in Fig. 1. The story heights of reference buildings are 3.2 m. The slab thickness is taken into account as 120 mm for all models. The weight of each slab was added

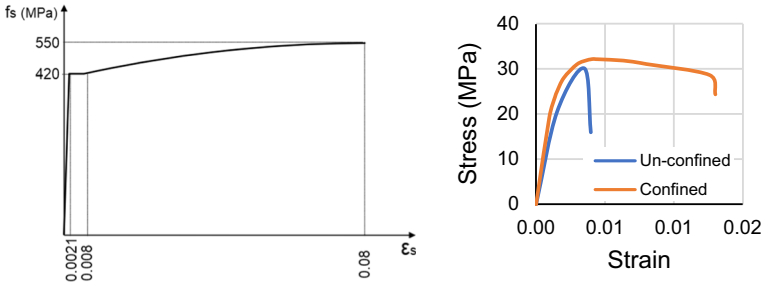


Fig. 1 Stress–strain relationship **a** reinforcement, **b** concrete and confined concrete

to the related beam members as 4.7 kN/m since the slabs are not considered as structural elements. Live load was selected 5 kN/m^2 (TS498 1997). The stiffness contribution of infill walls was ignored. Because Inel et al. (2008) has stated that the infill walls are more critical in low-rise reinforced concrete buildings composed of weaker members. However, used models in this study were designed with stronger reinforced concrete members respect to the most recent code TBEC-2018. Additionally, the infill walls are separated from the reinforced concrete frames at early stages of damages. For this reason, the stiffness contribution of infill walls was ignored, and infill walls were defined as the distributed load (3.25 kN/m) on the relevant beam elements. The buildings used in the study were assumed to be located near Pamukkale University in Denizli, Turkey on soil type ZC defined in TBEC-2018 which is similar to soil type C in FEMA-450 (FEMA-P-450 2003) for the design purposes. Longitudinal reinforcement ratios in the column members range between 1.00% and 1.15% which typical in Turkish building stock. Column and beam dimensions, reinforcement arrangement and axial force value are provided in Fig. 2. The design capacity principles that meet ductility conditions were adopted during the design phase. Additionally, interaction surfaces N-M_x-M_y of columns examples based on real values were given in the figure.

In order to reflect the nonlinear behavior on the model, firstly, moment–curvature analyzes were performed on the critical sections of the column and beam elements by using the SEMAp program. In the analyzes made using the Mander confined concrete model (1984), parameters such as the size of the sections, the content of longitudinal and transverse reinforcement and the level of axial load were used. Then, the rotation values calculated from the obtained curvature values were defined in the user-defined plastic hinge input interface of the SAP2000 program (SAP2000 CSI). The force–deformation relationship of a typical plastic hinge was given in Fig. 3. Detailed explanations of the points (A, B, C, D, E) defining this relationship were made in the study of Inel and Ozmen (2006). Additionally, IO, LS and CP correspond to Immediate Occupancy, Life Safety and Collapse Prevention performance levels, respectively. Finally, the defined plastic hinges were assigned to the relevant critical sections. Plastic hinges at column members were applied considering M_2-M_3 interaction since time history analyses performed as bi-directional. The effective section stiffness of column and beam members were defined 0.70EI and 0.35EI as defined in TBEC-2018 respectively. Since the structural members are designed according to the capacity design principles, shear hinge definition was not made.

Irregular structures were created by changing the distance between the centers of mass and the centers of rigidity of the reference models. The distance between the two centers is 20% of the length of the buildings in the y direction ($e_y = 0.2h$). The reason for the change being made only in the y direction is the idea that the eccentricity in the direction orthogonal to the collision direction of the buildings sequent in the x direction can better reflect the combination pounding and torsional amplifications. The column and beam element dimensions and vibration period values of the first 3 modes and, are given in Table 1 and the plan views of the models are given in Fig. 4. Additionally in the table, modal participating mass ratios (C_m) in translation and rotation direction show that the first mode is dominant and represents the significant part of structural response and deformations.

2.2 Adjacent models and link elements

Adjacent models were derived from different combinations of the regular and irregular structures. To represent the pounding (-p) and non-pounding (-np) situation, 2 cm and 4

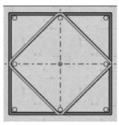
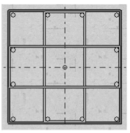
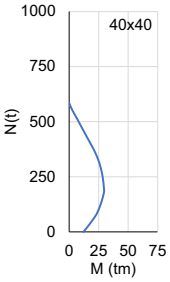
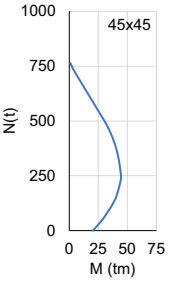
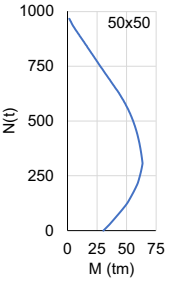
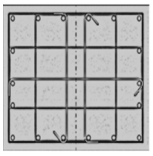
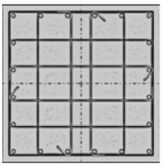
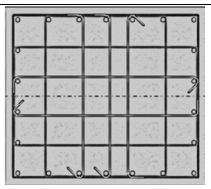
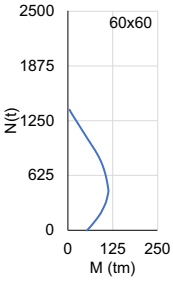
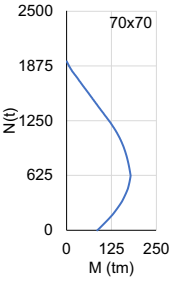
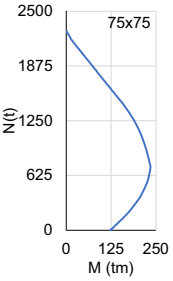
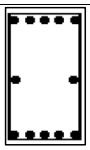
		
Column: 40 x 40 cm N= 374 kN 8ϕ16 Φ8/10/10	Column: 45 x 45 cm N= 799 kN 12ϕ16 Φ8/10/10	Column: 50 x 50 cm N= 467 kN 16ϕ16 Φ8/10/10
		
		
Column: 60 x 60 cm N= 461 kN 18ϕ18 Φ8/10/10	Column: 70 x 70 cm N= 826 kN 20ϕ20 Φ8/10/10	Column: 75 x 75 cm N= 1102 kN 22ϕ22 Φ8/10/10
		
 Beam: 30 x 50 cm N= 0 kN 12ϕ14 Φ8/15/10		

Fig. 2 Properties of sections and reinforcement of the structural members

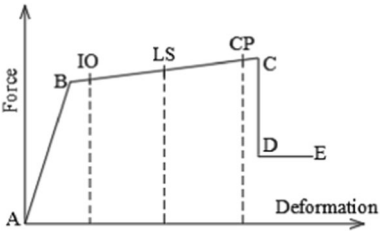


Fig. 3 Force–deformation relationship for a typical plastic hinge

Table 1 The dimensions of the carrier system element, dominant vibration period values and modal participating mass ratios for the models

Model	Regular 5-Story	Regular 9-Story	Irregular 5-Story	Irregular 9-Story
T_1 (s)	0.87	1.33	0.84	1.30
T_2 (s)	0.82	1.18	0.78	1.16
T_3 (s)	0.78	1.16	0.71	1.12
C_{m1}	0.8338	0.8085	0.8219	0.8012
C_{m2}	0.1034	0.0984	0.1075	0.1014
C_{m3}	0.0397	0.0388	0.0433	0.0400
Beam Elements (mm × mm)	300 × 500	300 × 500	300 × 500	300 × 500
Column Elements (mm × mm)	400 × 400	400 × 400 450 × 450 500 × 500	400 × 400 500 × 500 600 × 600	400 × 400 450 × 450 500 × 500 700 × 700 750 × 750

m gaps were left between the buildings, respectively. On the other hand, the effects of different sequences (row effect) of the same building models on seismic performance were evaluated by changing the places of the buildings relative to each other. Because frequency content of ground motion records differs significantly by time in each direction. When the positions of the building models are replaced by each other, the obtained results will also be different. To overcome this uncertainty, two different cases were considered for each adjacent building combination. In the first case, low- rise building model defined on the left side while high-rise one was on the right side. The placement of buildings was inverted in the second case. Each time history analysis was repeated for the cases. Additionally, the torsional effect was discussed for combinations of reference models without irregularity (e0) and combinations of models with irregularities. Besides, in combination of building models with irregularities, two different situations were created to examine the difference that may occur in case the positions of the building rigidity center (CR) change relative to each other. In the first of these, the centers of stiffness in both buildings are in the same direction and side (e20), and in the second, they are in the same direction but on different sides (e40). For the e40 combinations, instead of using a different building model, symmetrical according to the x-axis of the irregular 9-story model was used. In Fig. 5, the combinations of e0, e20 and e40 were given. CM and CR represent center of mass and center

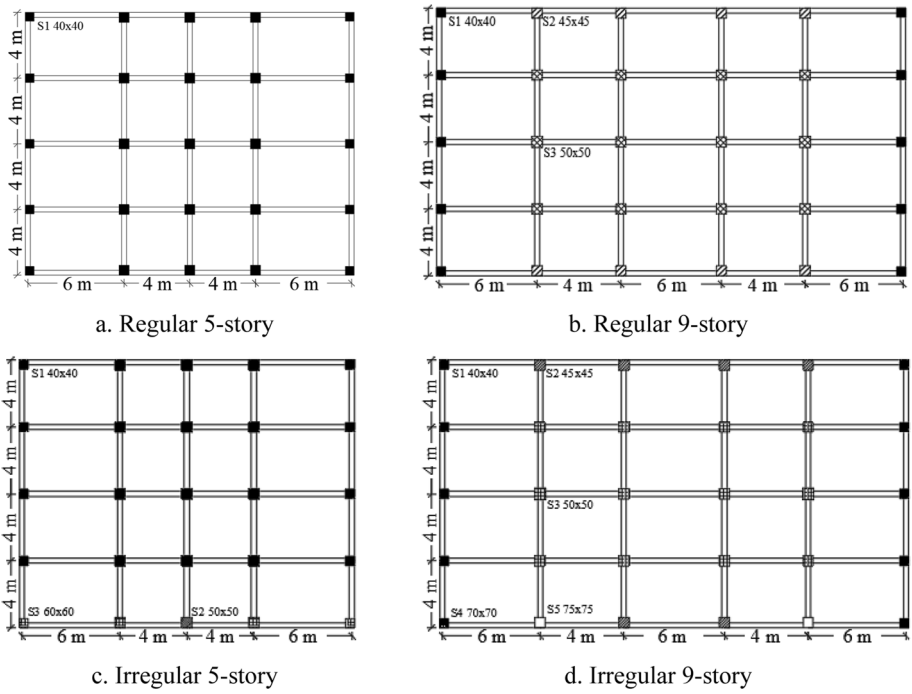


Fig. 4 Plan view of the considered buildings **a** regular 5-story, **b** regular 9-story, **c** irregular 5-story, **d** irregular 9-story

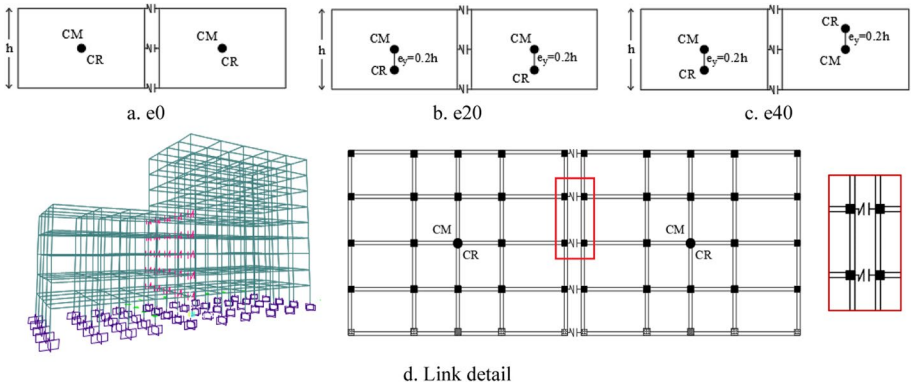


Fig. 5 Plan and three-dimensional view of the considered adjacent buildings **a** e0, **b** e20, **c** e40 and **d** link detail

of rigidity, respectively. The eccentricity in the y direction (e_y) is 20% of the building size (h) in this direction. Considering all conditions, the combination of pounding and torsion effects in adjacent models was evaluated for 2 different gap distances, 2 different building rows and 3 different eccentricities.

On the other hand, combination parameters of adjacent buildings are mentioned with a specific naming scheme throughout the text. When the gap distance between the buildings

is 2 cm, the pounding situation is expressed with "-p", and if the gap distance is 4 m, the non-pounding situation is expressed with "-np". If the 5-story model is on the left and 9-story model on the right "-59" and the opposite is expressed with "-95". Models were represented by “e0” if they consist of reference buildings without torsional irregularity. If the models consist of irregular buildings and the center of stiffness of these buildings is on the same side, they were represented by “e20”, and if they are on the different side, they were represented by “e40”. For example, p-e0-59; refers to the underlined 9-story model in the adjacent model, where there is a 2 cm gap between regular buildings 5-story on the left and 9-story on the right. Similarly, p-e20-59; refers to the underlined 5-story model in the adjacent irregular structure, where the centers of stiffness of irregular buildings 5-story on the left and 9-story on the right are on the same side and there is a 2 cm gap between the buildings. Also, np-e40-95; refers to the underlined 5-story model in the adjacent irregular structure, where the centers of stiffness of irregular buildings 9-story on the left and 5-story on the right are on the different side and there is a 4 m gap between the buildings.

Additionally, forced-base impact model details are given for adjacent buildings connected from column to column at the level of story slabs (Fig. 5). Although column to column connection methods are widely used in the literature (Flenga and Favvata 2021, 2023; Shakya and Wijeyewickrema 2009; Miari and Jankowski 2022), other impact models are developed like spatial impact model proposed to better investigate pounding effects (Mavronicola et al. (2017) In the spatial impact model the position of deformed structures is considered in modellig and determines the arbitrary location of the pounding point of the calculated impact forces based on the geometry near the impact (Polycarpou et al. 2014).

On the other hand, the Kelvin model components used in this study and shown in Fig. 6 consist of linear spring, viscous damping, and the gap distance defined between adjacent buildings (Muthukumar and Desroches 2004, 2006). If the clearance distance between the buildings is sufficient, the spring and damper will not work, so no force transfer will occur. However, if the gap between the buildings is insufficient, the viscous damping and the spring work under pressure (at the time of collision) and force transfer occurs between the buildings.

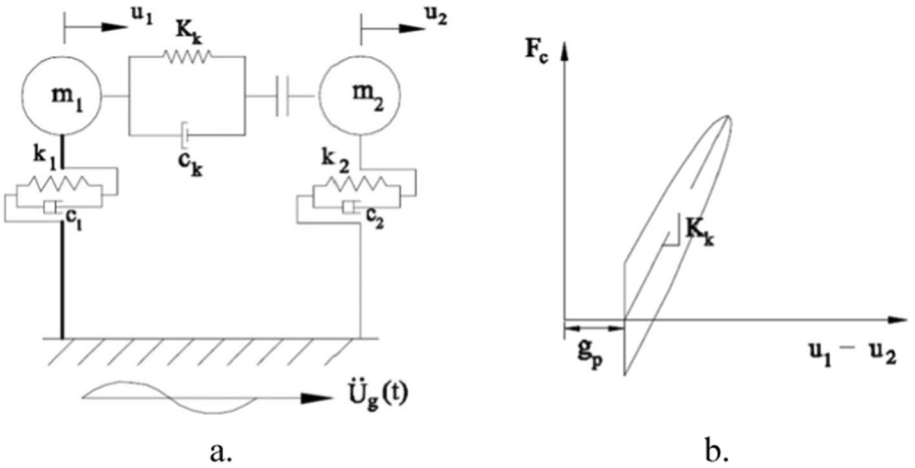


Fig. 6 Kelvin model (**a**) and force–deformation relationship (**b**) (Muthukumar and Desroches 2004, 2006)

The force on the link element is calculated according to Eqs. 1–3. The possible collisions occur at story levels as the adjacent buildings have the same story height. Since both buildings have rigid diaphragms, it is assumed that the collision occurs between two rigid bodies. Therefore, the spring stiffness (K_k) must be greater than the sum of the axial stiffnesses of the colliding stories (Muthukumar and Desroches 2004; Mahmoud and Jankowski 2011). In analytical and experimental studies dealing with concrete-to-concrete collision, spring stiffnesses were taken between about 1e10 and 1e11 N/m (Ghandil and Aldaikh 2017; Shakya and Wijeyewickrema 2009). In this study, the stiffness value was chosen as 1e10 N/m. In Eq. 2–3, c_k, K_k, e, m_1 and m_2 represent the viscous damping coefficient of link element, the spring stiffness, the energy efficiency coefficient, and the masses of the adjacent buildings, respectively (Anagnostopoulos 2004). In many studies, the coefficient e has been taken as 0.65 for concrete-to-concrete collision (Jankowski 2005; Cayci and Akpinar 2021). The damping ratio value (ξ) for this coefficient was obtained as 0.136. The maximum seismic weights for the 5-story and 9-story buildings were calculated as 32,623.2 kN and 12,753.8 kN, respectively. All of the link element properties were determined for these weights.

$$F = \begin{cases} K_k\left(u_1 - u_2 - g_p\right) + c_k\left(\dot{u}_1 - \dot{u}_2\right), \left(u_1 - u_2\right) \geq g_p \\ 0, \left(u_1 - u_2\right) < g_p \end{cases} \tag{1}$$

$$c_k = 2\xi\sqrt{K_k \frac{m_1 m_2}{m_1 + m_2}} \tag{2}$$

$$\xi = -\frac{\ln(e)}{\sqrt{\pi^2 + (\ln(e))^2}} \tag{3}$$

2.3 Torsional irregularity

One of the most common types of irregularities in buildings is torsional irregularity. This type of irregularity, which develops depending on the distance between the center of mass (CM) of the structure and the center of rigidity (RM), can cause unwanted vibration movements in the structure. Generally, in cases where the symmetrical layout of the structural system elements cannot be achieved (especially if the elevator bucket is surrounded by shear wall elements and the elevator bucket is far from the center of the building and the compensatory symmetry is not created in the building) it is highly likely to encounter this type of structural irregularity. Depending on the asymmetrical distribution, the relative drift values of the building corner points may move away from each other and exceed the limits allowed by the regulation as in Fig. 7.

The control parameter developed for torsional irregularity in TBEC-2018 is called the torsion coefficient (η_{bi}) and the irregularity coefficient is calculated according to Eqs. 4–5 (TBEC-2018). Parameters of $\Delta_{i,ma}k$, $\Delta_{i,min}$ and Δ_i in the formulas are represents the maximum, minimum and average relative story displacements at the story level i, respectively. If the coefficient calculated based on the relative story displacements is above the 1.2 limit value, there exists torsional irregularity in the building and the 5% additional eccentricity rate, which should be taken into account depending on the change in the live loads in the

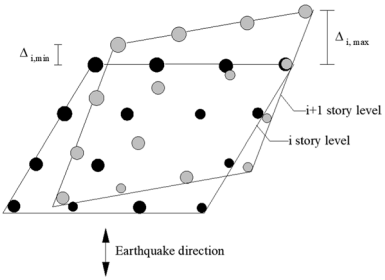


Fig. 7 Torsional irregularity case (TBEC-2018)

building, should be increased with a certain coefficient. If the calculated torsion coefficient is greater than 2, it may require a change in the calculation method used in the building design. In each step of the time-history analysis, the torsion coefficients were calculated in all models according to the relevant equations and the effects of torsion and pounding were interpreted.

$$\eta_{bi} = \frac{(\Delta_i)_{max}}{(\Delta_i)_{average}} > 1.2 \tag{4}$$

$$(\Delta_i)_{average} = \frac{(\Delta_i)_{max} - (\Delta_i)_{min}}{2} \tag{5}$$

3 Ground motion records

There are easily accessible databases for the real acceleration records used in the dynamic time history analysis method. In this study, Pacific Earthquake Engineering Research (PEER) database was used for the selection and scaling of earthquake records. While selecting and scaling, TBEC-2018 requirements were taken into consideration (TBEC-2018). In accordance with the building location and soil class, the design spectrum was obtained for earthquake with a probability of 10% to be exceeded in 475 years. In order to ensure the 3D time history dynamic analysis conditions in TBEC-2018, 1.3 times the design spectrum obtained was calculated and 11 pairs of ground motion records compatible with this spectrum were selected and scaled. It was attention that the number of ground motion and ground motion pairs to be selected for the same ground motion should not exceed three. Since the spectral matching method provides a more consistent, realistic, and less scattered average response with fewer number of ground motion recordings (Kayhan et al. 2011; Ozmen et al. 2019), the scaling process was performed using the spectral matching method. The same scale coefficient was applied to both horizontal components (H_1 and H_2) of the ground motion pairs. The average of the SRSS spectra of scaled ground motions was not less than 1.3 times the design spectrum in the $0.2T_p$ to $1.5T_p$ period range. The T_p represents the fundamental period of the structure. The properties of the selected and scaled ground motion records are given in Table 2. The obtained elastic acceleration

spectra for the 5% damping ratio and the average of the ground motion records are given in Fig. 8. Although the scatter of the selected records is high, the average values are very close to the TBEC-2018 spectrum requirement (1.3 times design spectrum). Additionally, both components of scaled ground motion pairs were applied to the building at the same time in the direction of the principal axes (0 and 90 degrees) respect to TBEC-2018 regulations. Then, the components were replaced with each other and again were applied at the same time in the principal axes to building. The obtained results were evaluated separately for both principal axis directions (*X, Y*).

4 Results and discussion

This study investigates the seismic behavior of adjacent buildings by considering pounding and torsion effects. The effect of gap distance between adjacent buildings, row arrangement of building and eccentricity were also investigated within the scope of seismic performance. A detailed comparison is made for adjacent models subjected to 11 pairs of spectrum-compatible ground motion. A total of 176 different nonlinear time history analyzes were performed for 8 different models. Within the scope of this study, many parameters such as displacement demands, interstory displacement demands, torsion coefficient, damage scatter and minimum distance to avoid collision were obtained and compared. The obtained maximum displacement values are normalized by building height while the maximum interstory displacement values are normalized by story height to obtain "roof drift ratio (RDR)" and "interstory drift ratio (IDR)" values, respectively. Although many pounding events were observed during the ground motion record, the values of the relevant parameters were determined for both pounding and non-pounding models for the moment when the maximum pounding (link) force was calculated. By choosing the same moment of the ground motion in pounding and non-pounding models, whether the impact restricts the displacement demands, changed how the interstory drift ratios with the effect of the pounding and the effect of torsion on this pounding are investigated. In addition, the change in damage distribution due to pounding and/or eccentricity and the minimum gap distance that should be left between buildings to prevent collision were also examined.

An example for the p-e0-95 model and RSN-302-90 ground motion recording is given in Fig. 9. Although many collision events were observed throughout the ground motion recording, the moment when the absolute maximum link force (F_{link}) was calculated was determined. Then, for this moment, displacement, interstory drift ratio and torsional coefficients of each adjacent buildings were calculated. On the other hand, since the link force calculated for non-pounding models is zero for all earthquake situations and models, the relevant calculations were made for the moment when the link force of the pounding model is maximum.

4.1 Evaluation of displacement demands

In order to evaluate the impact of pounding and eccentricity on the RDR demands, both separately and together, the demands of the pounding models were proportioned to the non-pounding models (pounding/non-pounding) and the demands of the irregular structures to the regular structures (e/e_0). The ratios of RDR values are shown in Fig. 10. In general, the average displacement demands of models with pounding increased in the x direction compared to the non-pounding model, while the change in the y direction

Table 2 Ground motion record properties used in the study (PEER)

No.	RSN	Earthquake	Year	Location	Mw	Componenet H_1-H_2	PGA (g)	Vs30 (m/s)	Scale Factor
1	88	San Fernando	1971	Santa Felita Dam	6.6	000–090	0.387	389.0	2.5
2	164	Imperial Valley-06	1979	Cerro Prieto	6.5	000–090	0.252	471.5	1.5
3	302	Irpinia_Italy-02	1980	Rionero In Vulture	6.2	000–270	0.399	574.9	4.0
4	313	Corinth_Greece	1981	Corinth	6.6	000–090	0.592	361.4	2.0
5	548	Chalfant Valley-02	1986	Benton	6.2	270–360	0.733	370.9	3.5
6	1614	Duzce_Turkey	1999	Lamont 1061	7.1	E-N	0.525	481.0	4.0
7	1633	Manjil_Iran	1990	Abbar	7.4	000–090	0.617	724.0	1.2
8	3750	Cape Mendocino	1992	Loleta Fire Station	7.0	270–360	0.531	515.7	2.0
9	3759	Landers	1992	Whitewater T.Farm	7.3	180–270	0.494	425.0	4.0
10	5815	Iwate_Japan	2008	Yuzawa	6.9	EW-NS	0.791	655.5	4.0
11	6915	Darfield_N.Zealand	2010	Heathcote V. PS	7.0	000–090	0.930	422.0	1.2

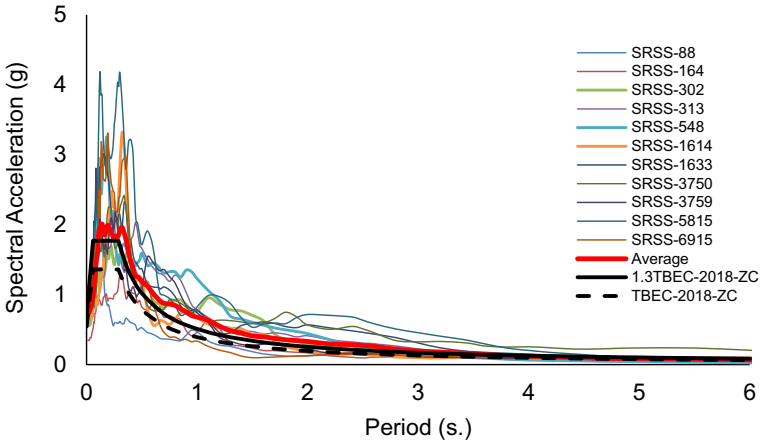


Fig. 8 Elastic acceleration spectrum for 5% damping of ground motion records used in the study

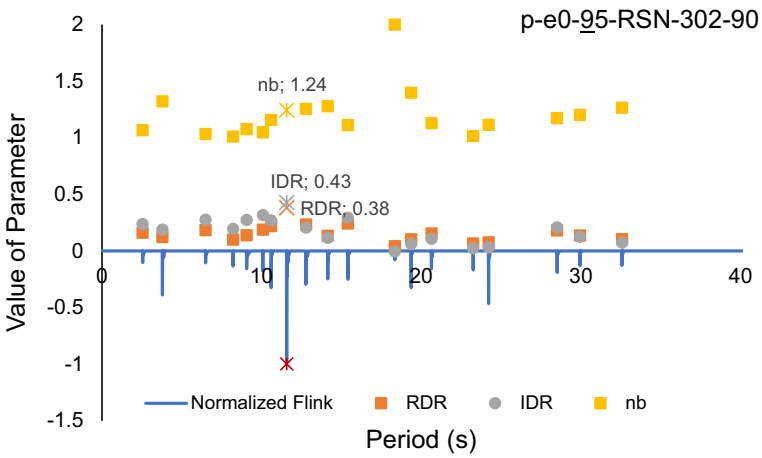


Fig. 9 Parameter values at the time of pounding

was negligible. Although the average displacement demands in the x direction have decreased in the e0-59 models among the 5-story models and the e40-95 models among the 9-story models, an increasing trend has been caught again when the building row of the same models has changed. When the building row is changed, the ratio of the displacement demand of the pounding model and the displacement demand of the non-pounding model varied the most for e40 buildings in the x direction (Fig. 10a, b). This change rate was determined as maximum of 24.1% and 31.5% for 5-story and 9-story buildings, respectively. The change in the building row and the pounding effect caused change of at most 6% in the y direction. While it was calculated in the x direction that the average displacement demands increased up to maximum 1.42 times with the effect of only pounding, it was determined that the displacement demands for individual ground motion could increase up to 6.23 times. However, in the y direction, the effect of

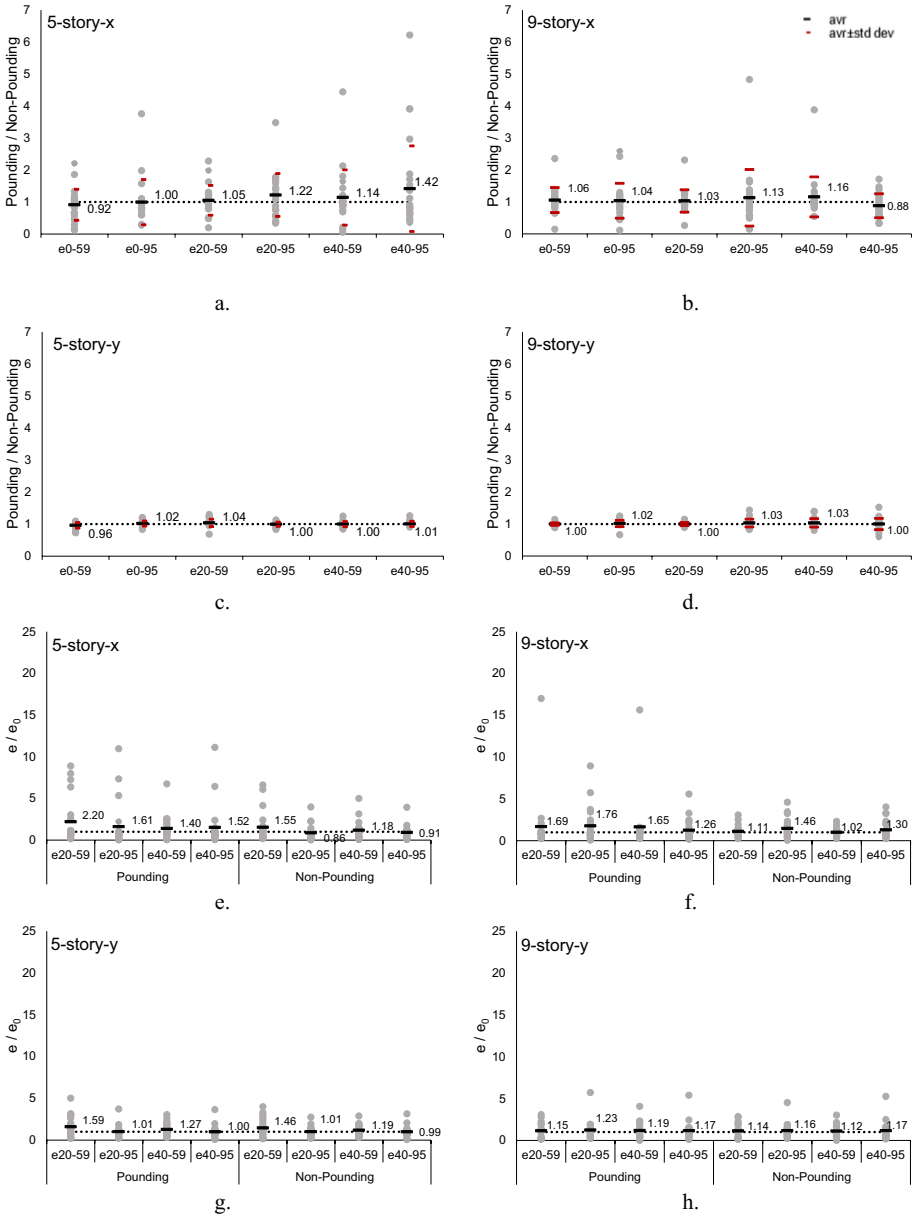


Fig. 10 Roof drift ratios of adjacent building models subjected to the scaled ground motion set

only pounding was negligible in most of the models both average values and individual ground motions. Because the highest average increase was 1.04 times in the 5-story e20 structure, and the least increase was calculated as 0.96 in the 5-story e0 model. For this reason, the changes in the y direction were quite limited compared to the changing rates in the x direction (Fig. 10a–d).

On the other hand, while one of the adjacent buildings is generally positively affected by the pounding behavior, the other may be negatively affected (Fig. 10a–d). For example, while a 5-story building is most sensitive to pounding and/or eccentricity effects in the e40-95 combination, the situation is the opposite for 9-story building. Similarly, while 9-story building is most sensitive to collision and/or eccentricity effects in the e0-59 combination, the situation is the opposite for 5-story building. However, while there is always a restriction in one, there may not be an increase in the other. For example, in the e40-59 combination, average demand values of both buildings increased compared to the non-pounding situation. For this reason, impact of pounding and/or eccentricity for each building combination respect to row arrangement, inelastic behavior, structural irregularities, scatter of damage etc. may be change. However, when a general evaluation is made, considering the standard deviation values along with the average values, it is possible to say that the shorter and less flexible structure are more sensitive to only pounding behavior.

In Fig. 10e–h different from these, only eccentricity increased the average displacement demands in all 9-story models while decreased in some of the 5-story models. In the non-pounding models (models with only eccentricity), the building row effect is not discussed. Because the difference in these models is independent of the row effect and is due to the difference in the seconds at which the maximum link force occurs. While only eccentricity increased the displacement demands up to 1.55 times on average in x-direction, it was observed that this increase may be up to 6.62 times for individual ground motion record. In addition, while only eccentricity in x-direction increased the displacement demands up to 1.46 times on average in y-direction, it was observed that this increase may be up to 5.27 times for individual ground motion record. The increase in maximum displacement values resulting only from eccentricity was calculated the most in e20 buildings.

When the effects of pounding and eccentricity are evaluated together, it is possible to say that all models cause increase in the calculated displacement demands for principal directions. With the combination of both effects, while the average displacement demands in x-direction increased up to 2.20 times, it was observed that this increase could be up to 17.02 times for each ground motion record. In addition, while the combination of both effects increased the displacement demands up to 1.59 times on average in y-direction, it was observed that this increase in y-direction may be up to 5.72 times for individual ground motion record. When the building row was changed, the average RDR demands changed up to 37.0% in the x direction and %57.1 in the y direction combination with the pounding and eccentricity effects. In addition, the highest increase in displacement demands due to eccentricity and pounding effects for both 5-story and 9-story models calculated in e20 models.

To summarize briefly, the RDR demand rates may decrease or increase with the only pounding effect or only torsional effect. It is seen that positive or negative effects may also occur depending on the characteristics of 22 ground motion. However, when both effects are evaluated together, RDR magnifications are more prominent especially in 5-story and e20 models. Additionally, the row arrangement of buildings affected RDR demands by up to 37% on average in critical direction. On the other hand, it should not be forgotten that a higher increase rate does not mean that the RDR demands are larger.

Since the displacement demands in Fig. 10 are calculated for the moment of collision, there is strong possibility that they may underestimate the impact of the pounding and/or eccentricity in terms of average values. The displacement in the direction of collision, which is generally expected to be decrease compared to non-pounding models, and Fig. 10 is generally the rate of demands at the time of restriction. For this reason, the average displacement values for pounding behavior in Fig. 10 shows partly meaningless influence of

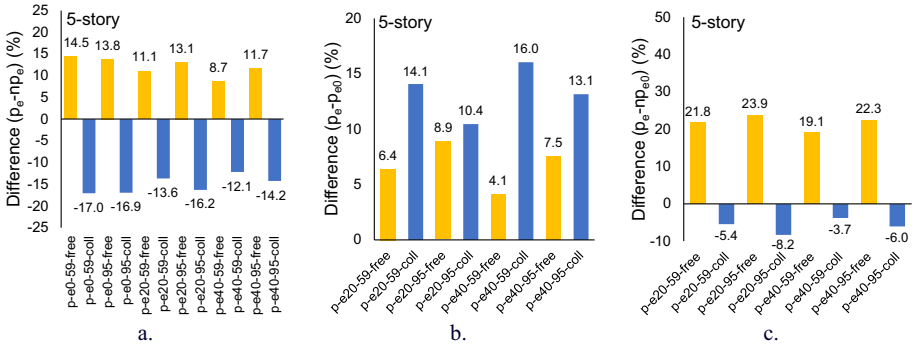


Fig. 11 The percentage displacement differences of the 5-story structures in the free direction and collision direction

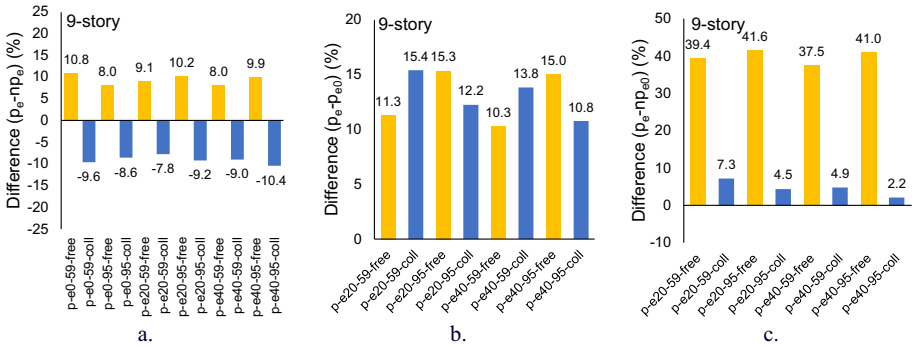


Fig. 12 The percentage displacement differences of the 9-story structures in the free direction and collision direction

the pounding and/or eccentricity effect between the examined adjacent structures. In order evaluate obtained results in detail, the absolute maximum displacement demands of the colliding buildings in the direction of free (free) and in the direction of collision (coll) were also calculated in Figs. 11 and 12. Figure 11a compares the case with pounding to the case non-pounding, while Fig. 11b compares the presence or absence of eccentricity in the case with pounding and Fig. 11c compares the case with pounding and eccentricity with the case non-pounding and non-eccentricity. Thus, how much the displacement demands of buildings in the collision and free directions decrease or increase is examined in more detail.

Accordingly, the increase (max 14%) in the displacement demands of 5-story models in the free direction due to pounding was less than the decrease (max 17%) in the collision direction (Fig. 11a). In the 9-story models, the increase (maximum 10.8%) and decrease (maximum 9.6%) rates were calculated to be closer to each other than in the 5-story model (Fig. 12a). However, it may express that in general, decrease of roof displacements in the collision direction was more severe than the increase in the free direction. Because the certain ratio of collision impact is absorbed with plastic deformations of structural members. Also, considering other parameters such as material damping, the collision momentum will not cause an equal increase in the free direction. In addition, the increase and decrease

rates in the 5-story models were greater than in the 9-story model (Figs. 11a and 12a). Therefore, it is possible to say that shorter and less ductile structures are more sensitive to pounding effects.

On the other hand, due to the eccentricity effect, the average displacement demands increased in both the free direction and the collision direction in all 5- and 9-story models (Figs. 11b and 12b). The highest difference between the increase rates in the free direction and in the collision-direction was calculated in the 5-story model as %290.2. In the 9-story model, the increase amounts in both directions were generally higher than 5-story and generally closer to each other. For this reason, the difference between the increase rates in the free direction and in the collision-direction is maximum %38.9. Although the certain ratio of increase in higher building might related with whiplash effect it is possible to say that longer and more ductile structures are more sensitive to eccentricity.

Figures 11c and 12c examine the changes in the average displacement demands in the free direction and in the collision direction in all p-e20 and p-e40 models, taking as reference the np-e0 models in which there is no collision and eccentricity. Accordingly, in 5-story models, displacement demands increased by an average of maximum 23.9% in the free direction due to both pounding and eccentricity effects, while they decreased by an average of 8.2% in the collision direction. In the 9-story model, displacement demands increased both in the collision direction and in the free direction. While the amount of increase reached 41.6% in the free direction, it was calculated as 7.3% in the collision direction. On the other hand, the increase rate in the displacement demands of the models due to both pounding and eccentricity effects was calculated at most in the 9-story model, while the decrease rate was calculated at most in the 5-story models. The results showed that if pounding and eccentricity effects are present at the same time, the shorter and more rigid building can be affected in a relatively in a positive way due to restriction, while the longer and more ductile building is affected relatively negatively.

4.2 Evaluation of IDR demands

The interstory drift ratio (IDR) is seen as an important indicator of possible damage to the building (Yang et al. 2010). Because, even if the building has made the same roof displacement according to the ground motion records, the distribution of the displacement demands on the interstory may vary. For this reason, it may be misleading to make an evaluation based on the roof displacement demands only.

Figure 13 compares of IDR ratios of pounding model/non-pounding model and irregular structure / regular structure. The IDR values calculated at all stories were determined at the maximum IDR story when at moment the link force was maximum. The IDR demands of all models in the x direction increased with the effect of only pounding, except for the 5-story regular structures and the highest average increase was 1.55 times in e40 structure for x direction. Additionally, it was determined that the IDR demands in the x direction for individual ground motion may increase up to 6.67 times. The change in the y direction was negligible compared to x direction. Because, while the highest average increase in the y direction was 1.04 times, it was maximum 1.95 times for individual ground motion (for 9-story e20 building). Further, some buildings were also decreased trend in average IDR values for y direction (Fig. 13a–d). When the building row was changed, the IDR demand rates of the pounding model compared to the non-pounding model changed maximum by 50.5% and 6.9% for the 5-story and 9-story models, respectively. This is an expected result

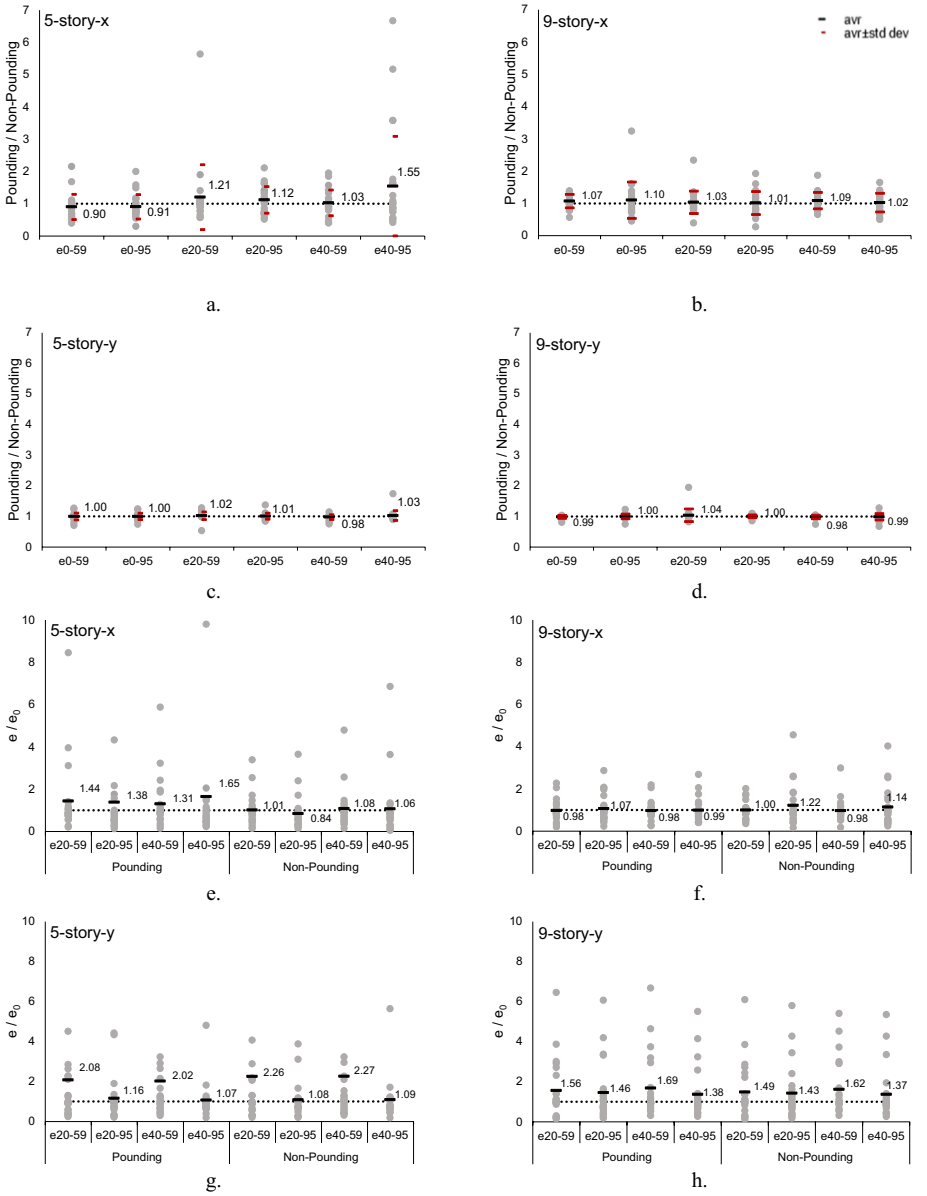


Fig. 13 Interstory drift ratios of adjacent building models subjected to the scaled ground motion set

considering that the shorter building is more sensitive to pounding behavior in adjacent structures.

On the other hand, the average IDR demands in case of only eccentricity increased for all models except the x direction of some models (Fig. 13e–h). The maximum average in the x direction compared to regular building was 1.22 times for e20 and 9-story structure, while it was calculated that this increase may be up to 6.86 times for each ground motion

record in the x direction. Additionally, the maximum average in the y direction compared to regular building was 2.27 times, while it was calculated that this increase may be up to 6.10 times for each ground motion record in the y direction. In the case of only eccentricity and considering that buildings are more sensitive for x-directional loading situations, it is thought that although the increase in the y direction is higher, the increases are not significant compared to the x direction. For this reason, considering the standard deviation values along with the average values, it is possible to say that 9-story models are more sensitive to eccentricity.

When the effect of pounding and eccentricity in the x direction are evaluated together, it is possible to say that all 5-story models caused an increase in the calculated IDR values. In 9-story models, on the other hand, a decreasing trend was observed in IDR values in general. Considering that the IDR demands generally have higher (critical) values in the lower stories, it is thought that this decrease is due to the fact that the 5-story model acts as a support for the 9-story model. On the other hand, when the effect of pounding and eccentricity in the y direction are evaluated together, it is possible to say that all 5-story and 9-story models caused an increase in the calculated IDR values. Because in this direction all of buildings are free (not restricted).

Additionally, the low-rise building usually subjected IDR amplifications on the pounding stories. With the combination of both effects, it was observed that while the IDR demands increased in the x direction maximum up to 1.65 times on average, this increase may be up to 10.77 times for each ground motion record. This increase ratio in the y direction was up to 1.04 times on average. For this reason, it is possible to say that the increase in IDR demands in the direction perpendicular to the collision is quite limited compared to those in the direction of the collision. When the building row was changed, the average IDR values increased maximum average 25.6% and maximum %79.3 for x direction. In addition, the highest increase in IDR demands, due to torsion and pounding effects, is calculated for the e20 models among both 5-story and 9-story models for the first five stories where the IDR are critical.

In order to better reveal the differences between the modeling approaches and both effects, the distribution of IDR values on each story is examined in Fig. 14. The relative drifts in the first five stories of the 9-story model reduced with support in the x direction while the upper stories increased significantly due to the whiplash effect. Although IDR values in the first five stories increased in the y direction, the increase ratios were limited with maximum average 1.03. The average maximum increase rate on the upper storys in the y direction increased to 1.06 times.

To summarize briefly, in terms of IDR values, shorter and more rigid buildings are generally negatively affected on the storys where collision occurs, while taller and more ductile buildings are more positively affected due to the restriction on these stories, which are critical in terms of IDR demands. However, on stories where there is no collision, the taller and more ductile building is exposed to greater drift demands due to pounding, torsion and whiplash effects. On the other hand, it is possible to say that the calculated IDR increases are more critical, especially for e20 models.

4.3 Torsional coefficient values

The ratio of the torsion coefficients calculated for all models according to the pounding and eccentricity conditions is given in Fig. 15. It has determined that the torsion coefficients due to the pounding effect increased in all models and both principal directions except the

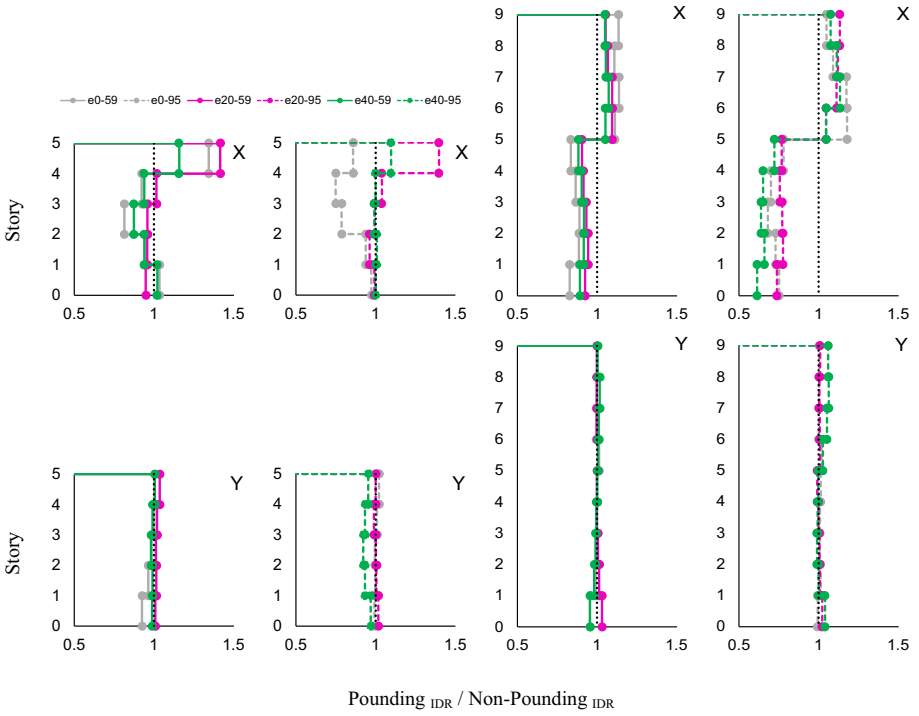


Fig. 14 Average interstory drift ratios along the height of adjacent building models in maximum pounding force

some 9-story structures (e0-95 model and e40-59 model). While the average maximum increase in the x direction with only pounding was up to 1.06 times, it is possible to say that it may be up to 2 times when evaluated separately for individual ground motion record. Additionally, the average maximum increase in the y direction with only pounding was up to 1.13 times, it is possible to say that it may be up to 2.79 times when evaluated separately for individual ground motion record. While the RDR and IDR parameters changed significantly with the effect of pounding only compared to the non-pounding condition, the torsion coefficient parameter showed a very limited change. For this reason, the changing ratio of torsion coefficient respect to building row arrangement also maximum limited with 13% for e20 model (Fig. 15a–d).

On the other hand, the torsion coefficient was increase in the x direction average up to 1.29 times with the increase in eccentricity only, it might be up to 2.11 times according to the ground motion record. In the y direction, the torsion coefficient was also increase average up to 1.28 times with the increase in eccentricity only, it might be up to 1.85 times according to the ground motion record.

Additionally, the torsional coefficient in the x direction by combined effect of pounding and eccentricity increased up to average of 1.24 times, and it increased up to 1.99 times according to the ground motion record. In the y direction, the torsion coefficient was also increase average up to 1.26 times with the increase in combined effect, it might be up to 1.93 times according to the ground motion record. When the building row was changed,

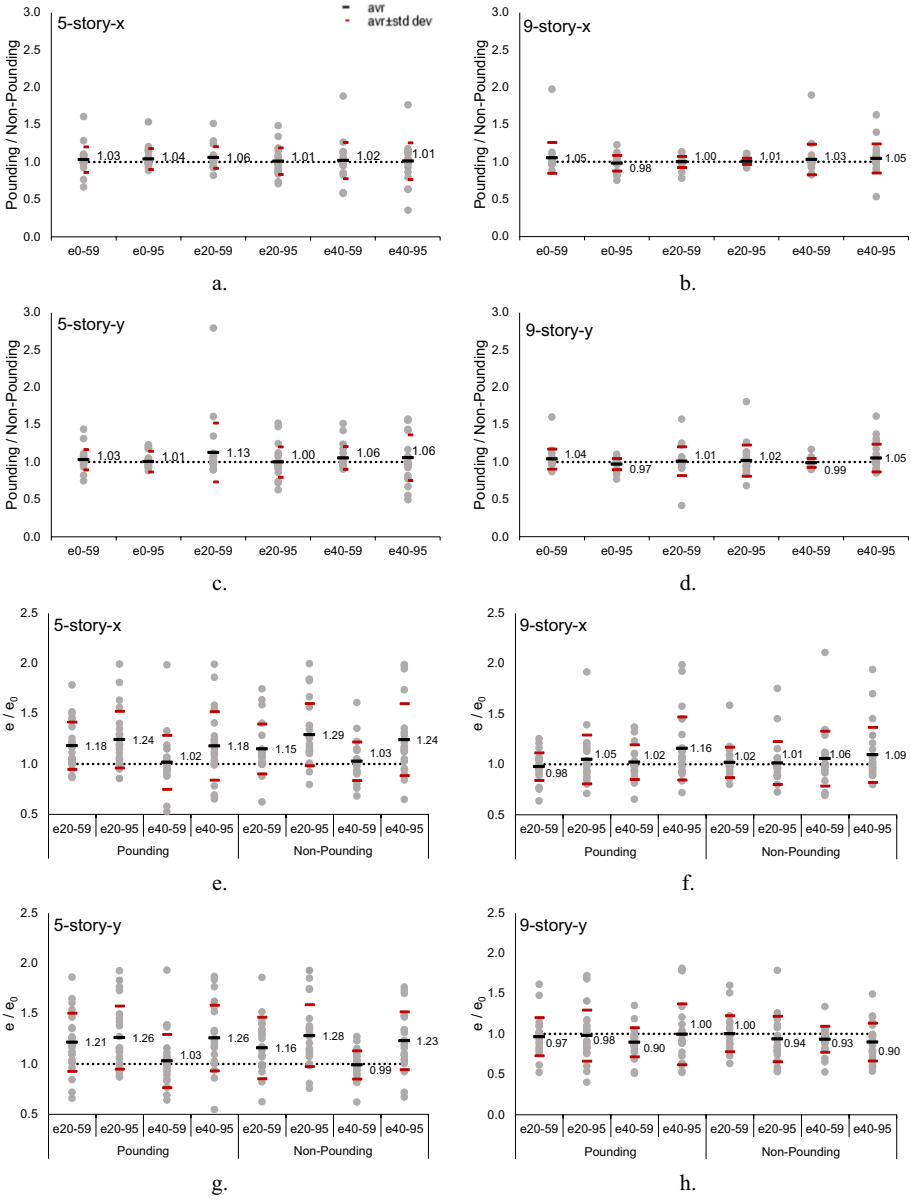


Fig. 15 Torsion coefficient ratios of adjacent building models subjected to the scaled ground motion set

the average torsion coefficient values maximum increased 15.7% for x direction and 22.3% for y direction (Fig. 15e–h).

In order to better reveal the differences between modeling approaches and both effects, the distribution of torsion coefficient values at each story is examined in Fig. 16. The torsion coefficient both principal directions generally increased. This increase was calculated as average maximum of 1.15 times and 1.16 times for the x and y directions, respectively.

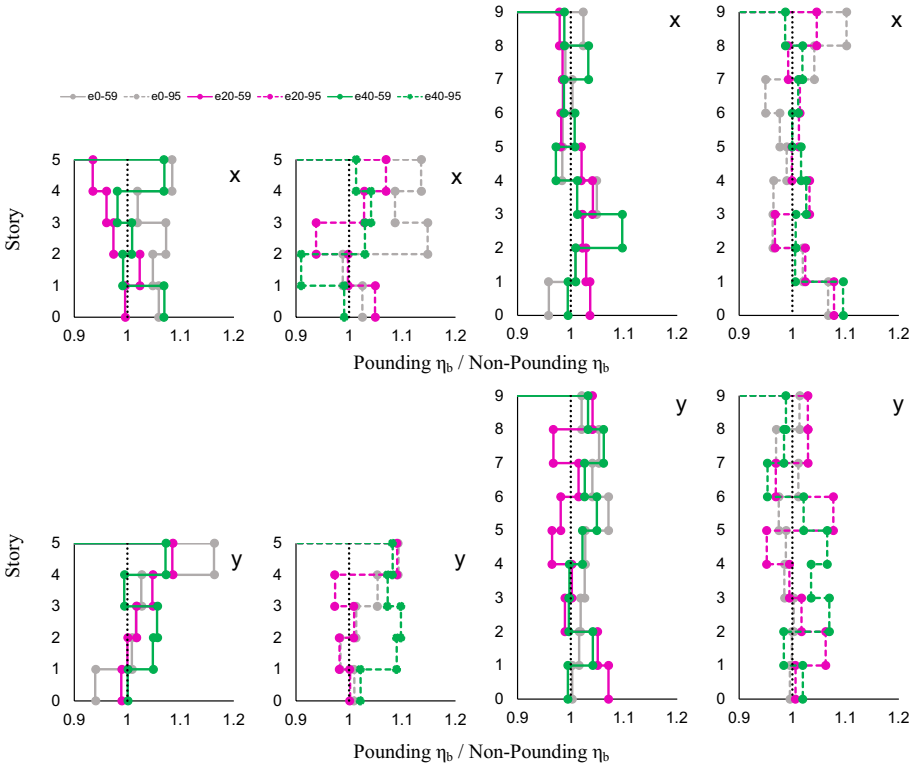


Fig. 16 Average torsion coefficient ratios along the height of adjacent building models in maximum pounding force

Besides these, how often the building is exposed to torsional behavior during the earthquake is another important point. The variation of the torsional irregularity coefficient for RDR and IDR history is given as an example for 9-story model -95 row and RSN-6915 record in Fig. 17 to better understand the combination effects of torsional irregularity and pounding on the seismic behavior. Since similar trends were observed in all ground motion records, these graphs were not given separately for all models. The calculated torsional coefficients exceeded the irregularity limit of 1.2 many times. There was insignificant difference in irregular structures for the non-pounding cases than the regular structure. However, in the case of pounding, both the RDR and IDR values in irregular structures (especially in the e20 model) increased remarkably, and the frequency of the torsion coefficient reaching 2 increased also. Thus, it has been seen more clearly that irregular structures are subject to torsional irregularity more frequently than regular structures, and that the most critical structure among irregular structure is e20 models.

Consequently, even if the change in torsion coefficient is limited to pounding and/or eccentricity effects, what is important is how often the building is exposed to torsion effects at a level that causes irregularity. Although the findings obtained from the study show a limited effect of only pounding on torsional coefficients, under the combination of eccentricity and pounding effects, buildings were exposed to torsion effects at a significant frequency, especially in e20 models.

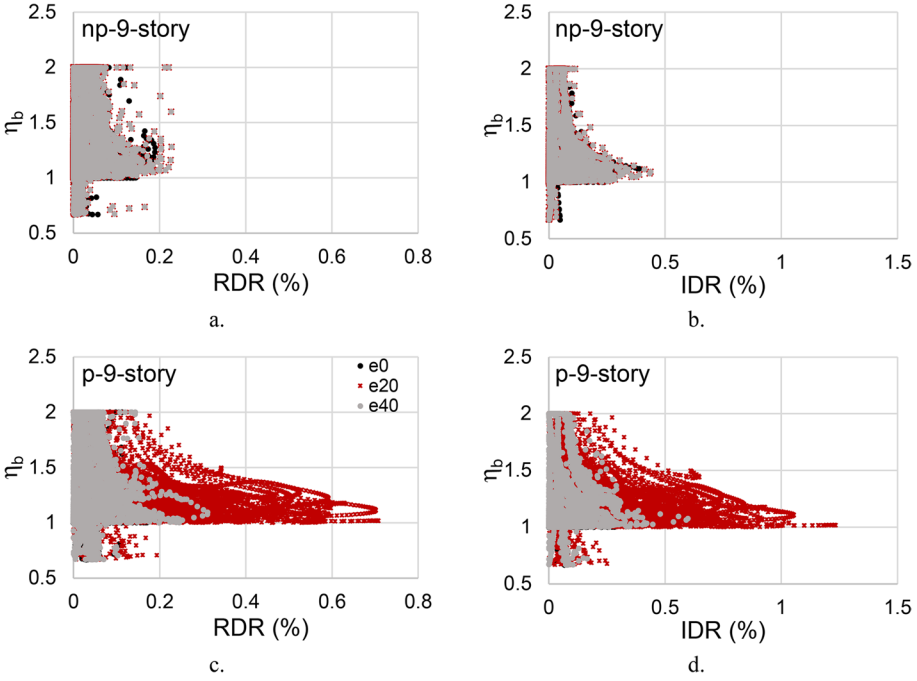


Fig. 17 Torsion coefficient (η_b) scatter for RSN-6915

4.4 Evaluation of damage scatter

Another parameter examined in the study was the effects of torsion and/or pounding behaviors on damage distribution. Plastic hinge damage state is useful indicator to investigate the demand level of each member of the structure (Cayci and Akpinar 2021). It is also a valuable tool to understand the damage mechanism for different dynamic inputs, as well as the diversity of pounding and/or eccentricity effects. In this aspect, plastic hinges used to consider the inelastic behavior of structural elements allowed observing the damage distribution under seismic loads. Thus, the effect of possible increases in local inelastic demand on structural elements under pounding and/or torsion effects on seismic performance was evaluated with a more realistic approach. Although the damage rate and distribution vary for individual ground motion records and building row arrangement, similar trends as were observed for building models considered in this study. For this reason, the change in damage distribution respect to models/effects was investigated through a selected example ground motion record (RSN-3759-90) and building row arrangement (95). While Fig. 18 shows the damage distribution in column members, Fig. 19 shows the damage distribution in beam members.

When a general evaluation is made, the column members of the reference models (np-e0) have reached the state of yielding (B-IO), mostly at the lower story levels. The upper story column members generally remained undamaged (elastic) (A-B). In case of only eccentricity or only pounding, the number of column members reaching the yield state and upper damage level (IO-LS) increased and the damage spread relatively towards the upper stories. Additionally, some column members of 9-story model were

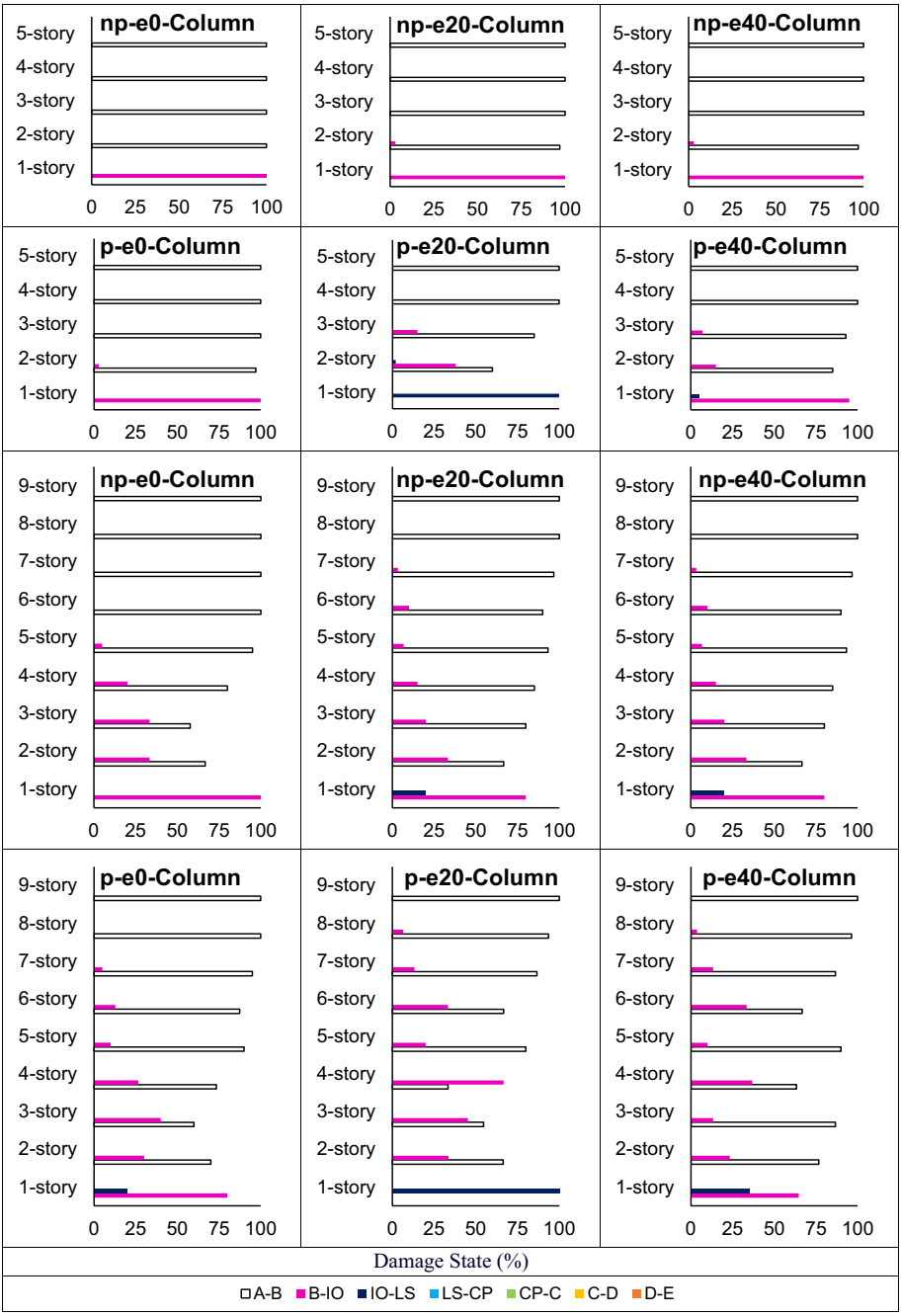


Fig. 18 Damage states of the column members for RSN-3759-90 ground motion record

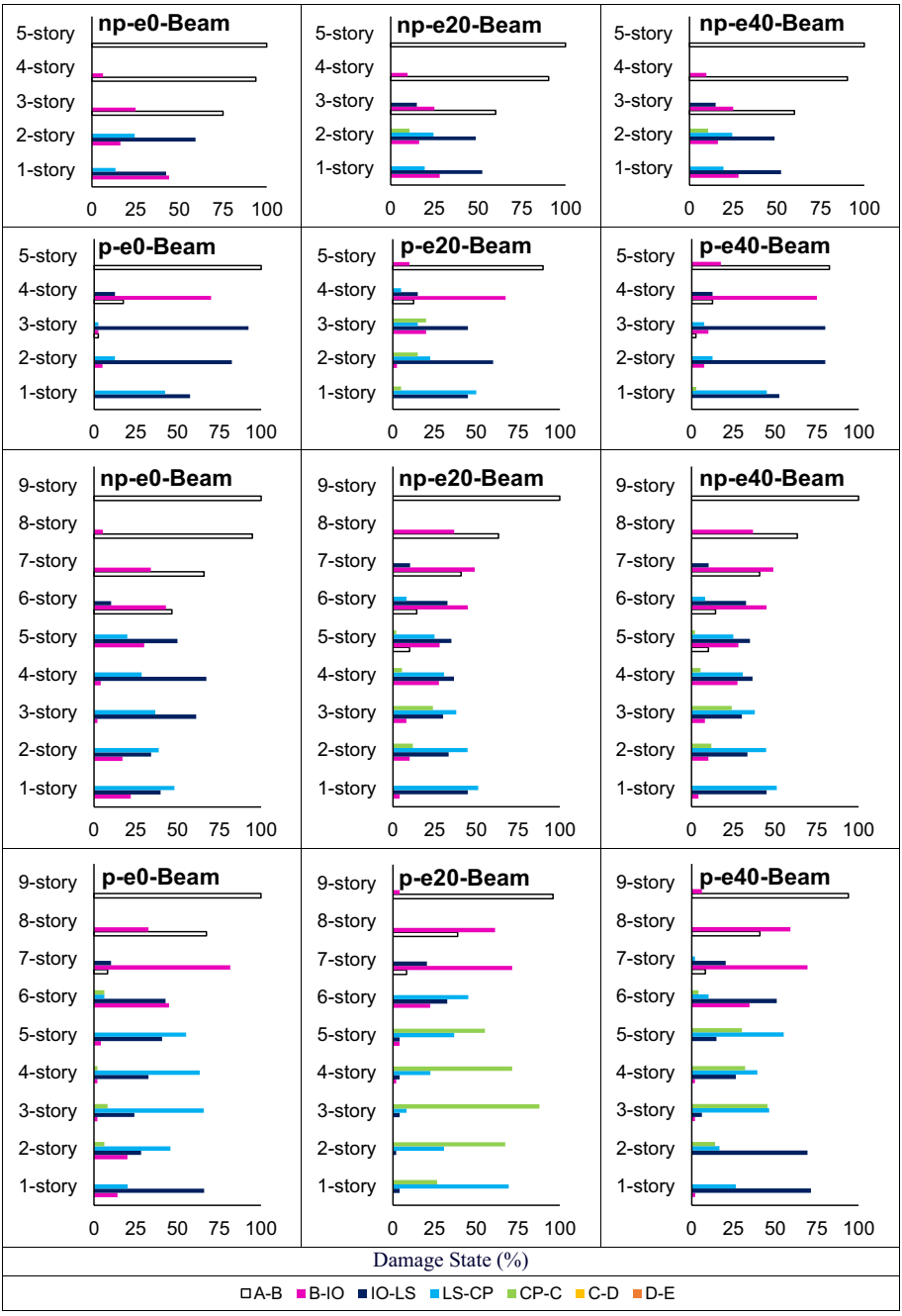


Fig. 19 Damage states of the beam members for RSN-3759-90 ground motion record

identified upper damage level (IO-LS) than yield level in case of only pounding and only eccentricity. In the case of both pounding and eccentricity, while all the bottom story column members for p-e20 models were reached an upper damage level (IO-LS), relatively less column members for p-e40 models were reached this level. Additionally, compared to the only eccentricity and only pounding cases and damage rate was increased even more. Moreover, it is possible to say that the damage to the column elements of 9-story models were increased relatively on the stories where the collision occurred, and especially on the 6th story. The reason for this increase observed on the 6th story can be expressed as the 5-story building acting as a support.

On the other hand, both the number of damaged elements and the level of damage have increased significantly in beam members compared to column members since strong column-weak beam behavior is considered in modelling stage. In case of only eccentricity or only pounding, both the damage rate and damage level of beam members increased respect to reference models, similar to the column members. While the damage distribution was generally concentrated in the lower stories in the case of only eccentricity, the damage was generally concentrated in the colliding stories levels in the case of only pounding and observed upper damage level in this story levels than others. While the highest damage level determined in the beam elements of the reference models was exceeded Life Safety damage level, where it was exceeded Collapse Prevention damage level in models with pounding and/or eccentricity. Especially in p-e20 models, there is a significant increase in the number of elements at exceed Collapse Prevention damage level compared to p-e40 models.

When the plastic hinge distributions in the pounding and/or eccentricity are examined, the differences in damage distribution between the models are obvious. Additionally, it was thought that the difference obtained when the percentage of damaged elements respectt to exceeding the total Life Safety and Collapse Prevention damage levels in the model/case examined, compared to the reference model/case, would provide a significant approximation. Therefore, in Table 3, the number of elements exceed the relevant damage levels is calculated as a percentage. For example, the Collapse Prevention damage level for beam elements of the 5-story e20 model was exceeded by 8.0% in the pounding model and 2.1% in the non-pounding model. Therefore, if the models are ranked from the most sensitive to the most stable for pounding and eccentricity effects, it is possible to express them as e20, e40 and e0. This result is similar to those obtained in the previous sections. On the other hand, it is possible to say that the

Table 3 Percentage difference of total damage compared to reference cases

Model		>CP				>LS			
		Pounding		Non-Pounding		Pounding		Non-Pounding	
		Column	Beam	Column	Beam	Column	Beam	Column	Beam
5-story	p-e0	0.00	0.00	0.00	0.00	0.00	5.75	0.00	3.80
	p-e20	0.00	8.00	0.00	2.10	0.00	13.25	0.00	5.45
	p-e40	0.00	0.50	0.00	2.10	0.00	6.75	0.00	5.45
9-story	p-e0	0.00	2.49	0.00	0.00	0.00	15.47	0.00	9.57
	p-e20	0.00	34.25	0.00	4.81	0.00	28.93	0.00	13.37
	p-e40	0.00	13.95	0.00	4.81	0.00	17.88	0.00	13.37

effects of pounding have greater share in the damage ratios in case of both pounding and eccentricity.

Consequently, differences in damage distributions were occurred in models under the influence of pounding and/or eccentricity due to the change in displacement demands and pounding forces. While the existence of only pounding or only eccentricity cases tend to increase local inelastic demands in general, most of structural members reached more critical damage levels when pounding and eccentricity effects considered together However, if inelastic behavior is neglected, it is not possible to observe member-based damage levels and collapse (damage) mechanism. Therefore, neglecting possible local inelastic effects may leads to non-conservative design or evaluation of structures that may become critical in some cases.

4.5 Minimum distance to avoid collision

To prevent collisions between adjacent buildings, the safe gap distance must be determined, and this distance must be applied on site. However, determining an exact distance becomes very difficult depending on many parameters such as the angle of impact of the earthquake on the building, frequency content, inelastic behavior of structural elements and torsion. On the other hand, while the determined gap distance may provide very conservative design for structures that are not expected to be exposed to serious seismic demands, the applicability of this distance remains very low, especially in city centers. Therefore, within the scope of the study, it was thought that instead of determining an exact gap distance to avoid a collision, it might be more logical to determine a sufficient distance at which collision effects are acceptable. For this purpose, models were used in which the link forces were calculated to be zero in all earthquake situations, so there was no collision, and there was distance of 4 m between them. In all relevant models, the maximum negative displacement values of the link elements were obtained. Since all obtained link deformation values are less than 4 m, it has been confirmed that there is no collision between the models. Then, the absolute maximum negative displacement values of link members and the average of these values for each model are given in Fig. 20 to develop an approach and create an idea.

The scatter of link deformations obtained depending on the frequency content of individual earthquake record sets is high (especially in e20 and e40 models). The required gap distance to prevent collision, which was up to 184.7 mm in the model without eccentricity (e0), reached 250.1 mm in the e20 model and reached 212.3 mm in the e40 model. However, considering that making an evaluation in terms of average values rather than

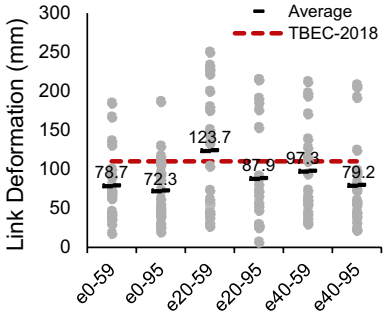


Fig. 20 Required gap distance values to avoid collision in average

individual records would develop a more realistic approach, average sufficient gap distances were also calculated. Accordingly, in terms of average values, the sufficient gap distance for the e0, e20 and e40 models was calculated as 78.7, 123.7 and 97.3 mm, respectively. When a general evaluation was made, it was concluded that leaving a gap of 124 mm would be sufficient, taking into account the torsional enlargements among the models used in the study. On the other hand, it was determined that torsional behavior increased the sufficient gap distance by 1.57 times on average compared to the regular structures. In addition, depending on the row (arrangement) of the buildings, the average sufficient gap distance varied at least 8.2% in e0 models and at most 28.9% in e20 models. This change rate, calculated depending on the building sequence in e40 models, was determined as 18.6%.

On the other hand, the gap distance that should be left between buildings according to Turkish Building Earthquake Code (TBEC 2018) regulation is found 11 cm between 5- and 9-story building models. It was concluded that this determined gap distance respect to TBEC-2018 regulation, considering the average link deformations, was insufficient for the e20-59 models. Additionally, this limit was exceeded in 28.8% of the analyses.

5 Conclusion

This study investigates the seismic behavior of adjacent buildings considering torsional irregularity and pounding effect for mid-rise reinforced concrete (RC) frame buildings with no shear walls. Torsional irregularity is reflected with static eccentricities due to distance between rigidity center and mass center of superstructure. Gap distance between buildings in the Kelvin link element model was selected 2 cm for pounding effect and 4 m for non-pounding effect. Furthermore, the building row effect was investigated by changing the location of adjacent buildings relative to each other. The nonlinear behavior of the structural members has been taken into account for observe the effects of torsional irregularity and pounding on the seismic behavior separately and together. For this purpose, 176 different nonlinear time history analyses of 3-dimensional 5 and 9-story models were performed considering 11 spectrum compatible ground motion record pairs. The remarkable outcomes are summarized below:

When the results are evaluated in general, pounding and/or torsional irregularity positive or negatively may affect the seismic performance and damage scatter of adjacent buildings depending by the row arrangement of buildings. The largest and critical values was obtained in terms of demand values, damage ratios and torsion coefficient are usually calculated in pounding models with torsional irregularity, when the eccentricity is in the same direction and side for both buildings. For this reason, when calculating sufficient gap distances in adjacent structures, the increase in demand values due to pounding and torsion effects should be taken into account and the adjacent buildings should be designed as regular as possible. In cases where this cannot be achieved, it is recommended that the neighboring building rigidity centers be on different sides. Additionally, the obtained results indicate that significant scatter exists in displacement demands of individual ground motion records for all models though this is not the case for average values. Similar to the previous studies, it is observed that frequency content of several ground motion records affects the dynamic response of the adjacent buildings. This study underlines the careful selection of number of ground motion records in dynamic analysis as mentioned in the literature. Moreover, the obtained results showed that neglecting possible local inelastic effects can lead to non-conservative design or evaluation of structures that may become critical in some cases.

On the other hand, it is thought that this study is important for design engineers and possible regulation changes. However, the study needs to be improved in future studies due to its limitations such as ignoring rotational vibrations caused by eccentric impact, not considered of soil-structure interaction, use of penetration depth and the low number and variety of models used. For these reasons, the detailing of the study subject for different building models, different eccentricity situations, different gap distance between buildings, and in the event of pounding of buildings, by forming an area instead of the depth of the penetration are suggested.

Acknowledgements Not applicable.

Author contributions Authors' contribution is equal.

Funding Open access funding provided by the Scientific and Technological Research Council of Türkiye (TÜBİTAK). The authors declare that no funds, grants, or other support were received during the preparation of this manuscript.

Availability of data and materials The datasets generated during and/or analysed during the current study are available from the corresponding author on reasonable request.

Code availability (software application or custom code) Not applicable.

Declarations

Conflict of interest The authors have no relevant financial or non-financial interests to disclose.

Ethical approval There is no conflict in this study.

Consent to participate Not applicable.

Consent for publication Not applicable.

Open Access This article is licensed under a Creative Commons Attribution 4.0 International License, which permits use, sharing, adaptation, distribution and reproduction in any medium or format, as long as you give appropriate credit to the original author(s) and the source, provide a link to the Creative Commons licence, and indicate if changes were made. The images or other third party material in this article are included in the article's Creative Commons licence, unless indicated otherwise in a credit line to the material. If material is not included in the article's Creative Commons licence and your intended use is not permitted by statutory regulation or exceeds the permitted use, you will need to obtain permission directly from the copyright holder. To view a copy of this licence, visit http://creativecommons.org/licenses/by/4.0/.

References

Abdel Raheem SE (2014) Mitigation measures for earthquake induced pounding effects on seismic performance of adjacent buildings. Bull Earthq Eng 12(4):1705–1724. https://doi.org/10.1007/s10518-014-9592-2

Anagnostopoulos SA (1988) Pounding of buildings in series during earthquakes. Earthq Eng Struct Dyn 16(3):443–456. https://doi.org/10.1002/eqe.4290160311

Anagnostopoulos SA (2004) Equivalent viscous damping for modeling inelastic impacts in earthquake pounding problems. Earthq Eng Struct Dyn 33(8):897–902. https://doi.org/10.1002/eqe.377

Barros RC, Naderpour H, Khatami SM, Mortezaei A (2013) Influence of seismic pounding on RC buildings with and without base isolation system subject to near-fault ground motions. J Rehabil Civ Eng 1:39–52. https://doi.org/10.22075/JRCE.2013.4

Cayci BT, Akpinar M (2021) Seismic pounding effects on typical building structures considering soil-structure interaction. In: Structures, vol 34. Elsevier, pp 1858–1871. https://doi.org/10.1016/j.istruc.2021.08.133

Chau KT, Wei XX, Shen CY, Wang LX (2004) Experimental and theoretical simulations of seismic torsional poundings between two adjacent structures. In 13th world conference on earthquake engineering 13WCEE, pp 1–6

Chau KT, Wei XX (2001) Pounding of structures modelled as non-linear impacts of two oscillators. Earthq Eng Struct Dyn 30(5):633–651. https://doi.org/10.1002/eqe.27

Cole G, Dhakal R, Carr AJ, Bull D (2010) Building pounding state of the art: Identifying structures vulnerable to pounding damage

Davis RO (1992) Pounding of buildings modelled by an impact oscillator. Earthq Eng Struct Dyn 21(3):253–274. https://doi.org/10.1002/eqe.4290210305

Degg MR (1992) Some implications of the 1985 Mexican earthquake for hazard assessment. Geohazards: Natural and man-made. Springer, Netherlands, Dordrecht, pp 105–114

Doğan M, Günaydin A (2009) Pounding of adjacent RC buildings during seismic loads. Eskişehir Osmangazi Üniversitesi Mühendislik Ve Mimarlık Fakültesi Dergisi 22(1):129–145

Efraimiadou S, Hatzigeorgiou GD, Beskos DE (2013) Structural pounding between adjacent buildings subjected to strong ground motions. Part I: The effect of different structures arrangement. Earthq Eng Struct Dyn 42(10):1509–1528. https://doi.org/10.1002/eqe.2285

Eurocode 8 (2004) Design of Structures for Earthquake Resistance - Part 1: General Rules, Seismic Actions and Rules for Buildings. European Committee for Standardization, Brussels

Farghaly AA (2017) Seismic analysis of adjacent buildings subjected to double pounding considering soil–structure interaction. Int J Adv Struct Eng 9(1):51–62. https://doi.org/10.1007/s40091-017-0148-y

Favvata MJ (2017) Minimum required separation gap for adjacent RC frames with potential inter-story seismic pounding. Eng Struct 152:643–659. https://doi.org/10.1016/j.engstruct.2017.09.025

Favvata MJ, Karayannis CG, Liolios AA (2009) Influence of exterior joint effect on the inter-story pounding interaction of structures. Struct Eng Mech 33:113–136. https://doi.org/10.12989/sem.2009.33.2.113

FEMA-P-450 (2003) Nehrp recommended provisions for seismic regulations for new buildings and other structures. Washington DC, USA

Fiore A, Marano GC, Monaco P (2013) Earthquake-induced lateral-torsional pounding between two equal height multi-storey buildings under multiple bi-directional ground motions. Adv Struct Eng 16(5):845–865. https://doi.org/10.1260/1369-4332.16.5

Flenga MG, Favvata MJ (2021) Probabilistic seismic assessment of the pounding risk based on the local demands of a multistory RC frame structure. Eng Struct 245:112789. https://doi.org/10.1016/j.engstruct.2021.112789

Flenga MG, Favvata MJ (2023) A risk-targeted decision model for the verification of the seismic performance of RC structures against structural pounding. Soil Dyn Earthq Eng 175:108229. https://doi.org/10.1016/j.soildyn.2023.108229

Freddi F, Padgett JE, Dall'Asta A (2017) Probabilistic seismic demand modeling of local level response parameters of an RC frame. Bull Earthq Eng 15(1):1–23. https://doi.org/10.1007/s10518-016-9948-x

Ghandil M, Aldaikh H (2017) Damage-based seismic planar pounding analysis of adjacent symmetric buildings considering inelastic structure–soil–structure interaction. Earthq Eng Struct Dyn 46(7):1141–1159. https://doi.org/10.1002/eqe.2848

Gong L, Hao H (2005) Analysis of coupled lateral-torsional-pounding responses of one-storey asymmetric adjacent structures subjected to bi-directional ground motions Part I: Uniform ground motion input. Adv Struct Eng 8(5):463–479. https://doi.org/10.1260/136943305774858043

Hao H, Shen J (2001) Estimation of relative displacement of two adjacent asymmetric structures. Earthq Eng Struct Dyn 30(1):81–96. https://doi.org/10.1002/1096-9845(200101)30:1%3c81::AID-EQE997%3e3.0.CO;2-E

Inel M, Ozmen HB (2006) Effects of plastic hinge properties in nonlinear analysis of reinforced concrete buildings. Eng Struct 28(11):1494–1502. https://doi.org/10.1016/j.engstruct.2006.01.017

Inel M, Ozmen HB, Bilgin H (2008) Re-evaluation of building damage during recent earthquakes in Turkey. Eng Struct 30:412–427. https://doi.org/10.1016/j.engstruct.2007.04.012

Jankowski R (2005) Non-linear viscoelastic modelling of earthquake-induced structural pounding. Earthq Eng Struct Dyn 34(6):595–611. https://doi.org/10.1002/eqe.434

Jankowski R (2009) Non-linear FEM analysis of earthquake-induced pounding between the main building and the stairway tower of the Olive View Hospital. Eng Struct 31(8):1851–1864. https://doi.org/10.1016/j.engstruct.2009.03.024

Jeng V, Tzeng WL (2000) Assessment of seismic pounding hazard for Taipei City. Eng Struct 22(5):459–471. https://doi.org/10.1016/S0141-0296(98)00123-0
Jiang S, Zhai C, Liu Y (2022) Experimental and numerical studies of seismic induced story-to-story and interstory pounding. Structures 46:555–569. https://doi.org/10.1016/j.istruc.2022.10.061
Jing HS, Young M (1991) Impact interactions between two vibration systems under random excitation. Earthq Eng Struct Dyn 20(7):667–681. https://doi.org/10.1002/eqe.4290200706
Jing W, Wang Q, Xing S, Cheng X, Song Y (2023) Control measures of collapse-pounding dynamic responses of adjacent structures under earthquake action. Soil Dyn Earthq Eng 165:107715. https://doi.org/10.1016/j.soildyn.2022.107715
Karayannis CG, Favvata MJ (2005a) Inter-story pounding between multistory reinforced concrete structures. Struct Eng Mech 20(5):505–526. https://doi.org/10.12989/sem.2005.20.5.505
Karayannis CG, Favvata MJ (2005b) Earthquake-induced interaction between adjacent reinforced concrete structures with non-equal heights. Earthq Eng Struct Dyn 34(1):1–20. https://doi.org/10.1002/eqe.398
Karayannis CG, Naoum MC (2018) Torsional behavior of multistory RC frame structures due to asymmetric seismic interaction. Eng Struct 163:93–111. https://doi.org/10.1016/j.engstruct.2018.02.038
Kayhan AH, Korkmaz KA, Irfanoglu A (2011) Selecting and scaling real ground motion records using harmony search algorithm. Soil Dyn Earthq Eng 31(7):941–953. https://doi.org/10.1016/j.soildyn.2011.02.009
Kuo PT (1974) Torsional effects in structures subjected to dynamic excitations of the ground. Ph.D. Thesis, Rice University
Leibovich E, Rutenberg A, Yankelevsky DZ (1996) On eccentric seismic pounding of symmetric buildings. Earthq Eng Struct Dyn 25(3):219–233. https://doi.org/10.1002/(SICI)1096-9845(199603)25:3%3c219::AID-EQE537%3e3.0.CO;2-H
Lopez-Garcia D, Soong TT (2009) Assessment of the separation necessary to prevent seismic pounding between linear structural systems. Probab Eng Mech 24(2):210–223. https://doi.org/10.1016/j.probengmech.2008.06.002
Mahmoud S, Jankowski R (2011) Modified linear viscoelastic model of earthquake-induced structural pounding. Trans Civ Environ Eng 35:51–62. https://doi.org/10.22099/IJSTC.2012.656
Mander JB (1984) Seismic design of bridge piers. Research report 84-2. Department of Civil Engineering, University of Canterbury, Christchurch (New Zealand)
Mavronicola EA, Polycarpou PC, Komodromos P (2017) Spatial seismic modeling of base-isolated buildings pounding against moat walls: effects of ground motion directionality and mass eccentricity. Earthq Eng Struct Dyn 46(7):1161–1179
Mavronicola EA, Polycarpou PC, Komodromos P (2020) Effect of ground motion directionality on the seismic response of base isolated buildings pounding against adjacent structures. Eng Struct 207:110202. https://doi.org/10.1016/j.engstruct.2020.110202
Mazza F, Labernarda R (2020) Magnetic damped links to reduce internal seismic pounding in base-isolated buildings. Bull Earthq Eng 18:6795–6824. https://doi.org/10.1007/s10518-020-00961-6
Mazza F, Labernarda R (2022) Effects of near-fault acceleration and non-acceleration pulses on pounding between in-plan irregular fixed-base and base-isolated buildings. Struct Cont Health Mon 29(9):e2992. https://doi.org/10.1002/stc.2992
Miari M, Jankowski R (2022) Analysis of floor-to-column pounding of buildings founded on different soil types. Bull Earthq Eng 20(13):7241–7262. https://doi.org/10.1007/s10518-022-01482-0
Miari M, Choong KK, Jankowski R (2019) Seismic pounding between adjacent buildings: Identification of parameters, soil interaction issues and mitigation measures. Soil Dyn Earthq Eng 121:135–150. https://doi.org/10.1016/j.soildyn.2019.02.024
Mouzakis HP, Papadrakakis M (2004) Three dimensional nonlinear building pounding with friction during earthquakes. J Earthq Eng 8(01):107–132. https://doi.org/10.1142/S1363246904001353
Muthukumar S, Desroches R (2004) Evaluation of impact models for seismic pounding. In: 13th world conference on earthquake engineering, Vancouver, BC, Canada, 235, August 1–6, 2004
Muthukumar S, DesRoches R (2006) A Hertz contact model with non-linear damping for pounding simulation. Earthq Eng Struct Dyn 35:811–828. https://doi.org/10.1002/eqe.557
Naderpour H, Khatami SM, Barros RC (2017) Prediction of critical distance between two MDOF systems subjected to seismic excitation in terms of artificial neural networks. Period Polytech: Civ Eng 61(3):516–529. https://doi.org/10.3311/PPci.9618
Ozmen HB, Yilmaz H, Yildiz H (2019) An acceleration record set for different frequency content, amplitude and site classes. Res Eng Struct Mater 5(3):321–333. https://doi.org/10.17515/resm2019.116ea0209ds
Pacific Earthquake Engineering Research Center (PEER) (2019) Ground Motion Database. http://ngawest2.berkeley.edu/. 2019. Accessed 19.05.2019

Pant DR, Wijeyewickrema AC (2012) Structural performance of a base-isolated reinforced concrete building subjected to seismic pounding. Earthq Eng Struct Dyn 41(12):1709–1716. https://doi.org/10.1002/eqe.2158

Papadrakakis M, Apostolopoulou C, Zacharopoulos A, Bitzarakis S (1996) Three-dimensional simulation of structural pounding during earthquakes. J Eng Mech 122(5):423–431. https://doi.org/10.1061/(ASCE)0733-9399(1996)122:5(423

Polycarpou PC, Papaloizou L, Komodromos P (2014) An efficient methodology for simulating earthquake-induced 3D pounding of buildings. Earthq Eng Struct Dyn 43(7):985–1003. https://doi.org/10.1002/eqe.2383

Rayegani A, Nouri G (2022) Application of smart dampers for prevention of seismic pounding in isolated structures subjected to near-fault earthquakes. J Earthq Eng 26(8):4069–4084. https://doi.org/10.1080/13632469.2020.1822230

Rosenblueth E, Meli R (1986) The 1985 Mexico earthquake. Concrete Int 8:23–34

SAP (2000) CSI (2020) Integrated software for structural analysis and design. Computers and Structures Inc., Berkeley

SEMAp Sargı Etkisi Modelleme Analiz Programı (2008) Tubitak Proje No: 105M024 Ankara, Turkey (in Turkish)

Shakya K, Wijeyewickrema AC (2009) Mid-column pounding of multi-story reinforced concrete buildings considering soil effects. Adv Struct Eng 12(1):71–85. https://doi.org/10.1260/136943309787522687

Tabatabaei R (2011) Torsional vibration of eccentric building systems (pp. 169–192). InTech.

Turkish Building Earthquake Code (TBEC-2018) (2018) Republic of Turkey Prime Ministry Disaster and Emergency Management Authory Presidential of Earthquake Department. Ankara, Turkey (in Turkish)

TS498 (1997) Design Loads for Buildings. Turkish Standards Institution. Ankara, Turkey.

Wada A, Shinozuka Y, Noriyoshi N (1984) Collapse of building with expansion joints through collision caused by earthquake motion.

Wang LX, Chau KT, Wei XX (2009) Numerical simulations of nonlinear seismic torsional pounding between two single-story structures. Adv Struct Eng 12(1):87–101. https://doi.org/10.1260/136943309787522267

Wei XX, Wang LX, Chau KT (2009) Nonlinear seismic torsional pounding between an asymmetric tower and a barrier. Earthq Spectra 25(4):899–925. https://doi.org/10.1193/1.3207177

Yang TY, Konstantinidis D, Kelly JM (2010) The influence of isolator hysteresis on equipment performance in seismic isolated buildings. Earthq Spectra 26(1):275–293. https://doi.org/10.1193/1.3276901

Ye K, Li L, Zhu H (2009) A modified Kelvin impact model for pounding simulation of base-isolated building with adjacent structures. Earthq Eng Eng Vib 8:433–446

Zhai C, Jiang S, Li S, Xie L (2015) Dimensional analysis of earthquake-induced pounding between adjacent inelastic MDOF buildings. Earthq Eng and Eng Vib 14:295–313. https://doi.org/10.1007/s11803-015-0024-3

Publisher's Note Springer Nature remains neutral with regard to jurisdictional claims in published maps and institutional affiliations.